Coupling between Arctic feedbacks and changes in poleward energy transport

Yen-Ting Hwang,[1] Dargan M. W. Frierson,[1] and Jennifer E. Kay[2]

Received 8 July 2011; revised 15 August 2011; accepted 15 August 2011; published 10 September 2011.

[1] The relationship between poleward energy transport and Arctic amplification is examined using climate models and an energy balance model. In 21st century projections, models with large Arctic amplification have strong surface albedo and longwave cloud feedbacks, but only weak increases (or even decreases) in total energy transport into the Arctic. Enhanced Arctic warming weakens the equator-to-pole temperature gradient and decreases atmospheric dry static energy transport, a decrease that often outweighs increases from atmospheric moisture transport and ocean heat transport. Model spread in atmospheric energy transport cannot explain model spread in polar amplification; models with greater polar amplification must instead have stronger local feedbacks. Because local feedbacks affect temperature gradients, coupling between energy transports and Arctic feedbacks cannot be neglected when studying Arctic amplification.
Citation: Hwang, Y.-T., D. M. W. Frierson, and J. E. Kay (2011), Coupling between Arctic feedbacks and changes in poleward energy transport, *Geophys. Res. Lett.*, *38*, L17704, doi:10.1029/2011GL048546.

1. Introduction

[2] Polar amplification is a robust climate response in CO_2-forced warming simulations; however, there is a large spread in the modeled amplification amount. In the Coupled Model Intercomparison Project Phase 3 (CMIP3), the increase in Arctic temperature poleward of 70N ranges from 3.6 K to 8.0 K for the A1B scenario for 2081-2100 relative to 2001–2020, whereas the global mean projects ranges from 1.9 K to 3.3 K (Table 1). There have been many proposed mechanisms to explain this enhanced warming in the Arctic, involving both local processes and changes in poleward energy transports.

[3] Surface albedo feedback was the first proposed mechanism for polar amplification [*Sellers*, 1969; *Manabe and Stouffer*, 1980; *Hall*, 2004]. Longwave cloud and lapse rate feedbacks have also been shown to contribute to polar amplification [*Hall*, 2004; *Graversen and Wang*, 2009; *Boe et al.*, 2009], and these increases in downward longwave can be even more important than surface albedo feedback [*Winton*, 2006]. In terms of energy transport, increasing moisture transport in a warmer climate was found to be responsible for enhanced Arctic warming in idealized experiments without surface albedo feedback [*Hall*, 2004; *Alexeev et al.*, 2005; *Graversen and Wang*, 2009]. Also, increasing oceanic transport is correlated with Arctic warming and the amount of sea ice loss [*Holland and Bitz*, 2003; *Bitz et al.*, 2006; *Holland et al.*, 2006; *Mahlstein and Knutti*, 2011].

[4] Currently there is no consensus on the main process of polar amplification or the main reason for model spread. Evaluating the relative importance of individual mechanisms is challenging from a modeling perspective, as most mechanisms are strongly coupled. As mentioned by J. E. Kay et al. (The influence of local feedbacks and northward heat transport on the equilibrium arctic climate response to increased greenhouse gas forcing in coupled climate models, submitted to *Journal of Climate*, 2011), suppressed surface albedo feedback experiments may overestimate the effect of energy transport on Arctic amplification, as such experiments do not include the decreasing dry static energy transport response to surface albedo feedback. In this study, we focus on the coupled relationship between local feedbacks in the Arctic and the energy that is transported into the Arctic, a key relationship that cannot be neglected when interpreting results of modeling experiments.

2. Changes in Poleward Energy Transport

[5] *Trenberth and Fasullo* [2010] compared the base-state poleward energy transport from 1990 to 1999 in CMIP3 models with observations. Here, we calculate changes of these transports with global warming as the mean from 2081-2100 minus the mean from 2001–2020 in each scenario. As listed in Table 1, ten models in the A1B scenario and ten models in the A2 scenario are considered, because they supplied the necessary data for the analysis. The results in the A1B scenario are qualitatively similar with the A2 scenario, so we only show the results from the A2 scenario in some of the figures.

2.1. Atmospheric Energy Transport: Moisture Transport and Dry Static Energy Transport

[6] The changes in northward atmospheric energy transport in the A2 scenario are plotted in Figure 1a, colored in order of their change at 70N. The change in atmospheric energy transport can be separated into moisture and dry static energy (DSE) transport changes (Figure 1b) (see *Overland et al.* [1996] for equations). All of the models project increasing moisture transport, due to increases in water vapor content as the climate warms [*Held and Soden*, 2006; *Solomon*, 2006]. Increasing moisture content causes most of the increase in poleward energy transport in mid-latitudes [*Hwang and Frierson*, 2010]; however, this increase is significantly smaller in high latitudes where the nonlinearity of Clausius-Clapeyron causes the water vapor content not to increase as much. At 70N, the increase in moisture transport is about

[1]Department of Atmospheric Sciences, University of Washington, Seattle, Washington, USA.
[2]Climate and Global Dynamics Division, National Center for Atmospheric Research, Boulder, Colorado, USA.

0094-8276/11/2011GL048546

Table 1. List of Models and their Arctic Temperature Change, Global Mean Temperature Change, and Polar Amplification

Models	Arctic Temperature Change (Poleward Than 70N) (K)	Global Mean Temperature Change (K)	Polar Amplification
	A1B Scenario		
CCCMA CGCM3 (T47)	3.84	1.89	2.03
GFDL CM2.0	4.66	2.30	2.03
GFDL CM2.1	4.18	1.94	2.15
INM CM3	3.59	1.88	1.90
MIROC (medres)	7.25	2.71	2.67
MIROC (hires)	7.21	3.32	2.17
MPI ECHAM5	6.67	2.84	2.34
MRI CGCM2	4.50	1.94	2.32
NCAR CCSM3	5.76	1.91	3.02
UKMO Hadgem1	7.97	2.69	2.96
Multi-model mean	**5.56**	**2.34**	**2.36**
	A2 Scenario		
CCCMA CGCM3 (T47)	5.64	2.69	2.09
CNRM CM3	7.23	2.92	2.48
GFDL CM2.0	4.62	2.69	1.71
INM CM3	4.86	2.55	1.90
MIROC (medres)	8.28	2.97	2.79
MPI ECHAM5	7.36	3.09	2.38
MRI CGCM2	5.49	2.22	2.47
NCAR CCSM3	7.81	2.80	2.78
UKMO Hadgem1	9.65	3.16	3.05
UKMO HadCM3	6.54	2.94	2.23
Multi-model mean	**6.75**	**2.80**	**2.39**

0.05 PW, corresponding to ~3.2 W/m^2 of heating poleward of 70N. The decrease in DSE transport dominates the inter-model spread of total atmospheric transport. Thus, models that project large decreases in DSE transport (blue dash lines in Figure 1b) also produce decreasing atmospheric energy transport at 70N (blue solid lines in Figure 1a).

2.2. Changes in Oceanic Energy Transport

[7] We approximate the implied oceanic energy transport from the surface energy imbalance as in Figure 8.6 of *Intergovernmental Panel on Climate Change* [2007]. This estimate includes ocean heat uptake and latent heat fluxes from melting and forming ice. Only a limited subset of models includes ocean energy transport in the CMIP3 archive [*Holland et al.*, 2010; *Mahlstein and Knutti*, 2011], therefore we use this approximate method to include more models in this model comparison study. Most models project a decrease in oceanic energy transport in midlatitudes and an increase in higher latitudes (Figure 1c). The decrease in midlatitudes is mainly associated with a weaker meridional overturning circulation in North Atlantic [*Gregory et al.*, 2005; *Cunningham and Marsh*, 2010]. The mechanisms for the increase in ocean heat flux in high latitudes are not fully understood, although *Bitz et al.* [2006] suggest that such increases are associated with changing ice thickness. Ice production in central Arctic and Siberian shelves increases as the ice gets thinner, and the production of ice drives ocean ventilation and strengthens the inflow of warm Atlantic waters. The significance of this effect depends on time. *Holland et al.* [2010] suggest that the change in ocean energy transport becomes more important toward the end of the 21st century. Figure 1c is colored in the same order as Figure 1a, showing that models with larger increases in oceanic transport are also the models that project a larger decrease in atmospheric transport. The two transports compensate each other [*Held and Soden* [2006] (see also the correction of *Hwang et al.* [2011]), with the changes in the atmospheric transport being larger than the changes in the ocean.

2.3. Anticorrelation Between Energy Transports and Polar Amplification

[8] Table 2 contains the correlation coefficient between changes in energy transports and the amount of polar amplification, which is defined as the increase in 2 m air temperature poleward of 70N normalized by the change in global mean temperature in each GCM. The increasing atmospheric energy transport is negatively correlated with polar amplification (as shown in Figure 2a). Models with high polar amplification project little increase or even a decrease in the atmospheric energy transport. The DSE

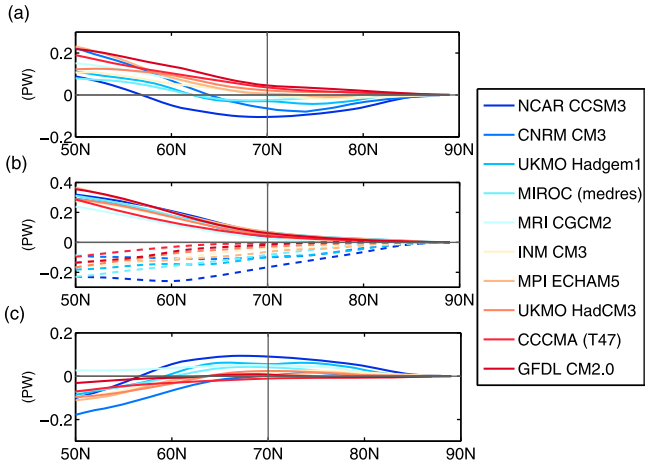

Figure 1. Changes in northward energy transports in PW from 2001~2020 to 2081 ~2100 in the A2 Scenario: (a) atmospheric energy transport, (b) moisture (solid) and DSE (dashed) transport, and (c) oceanic energy transport.

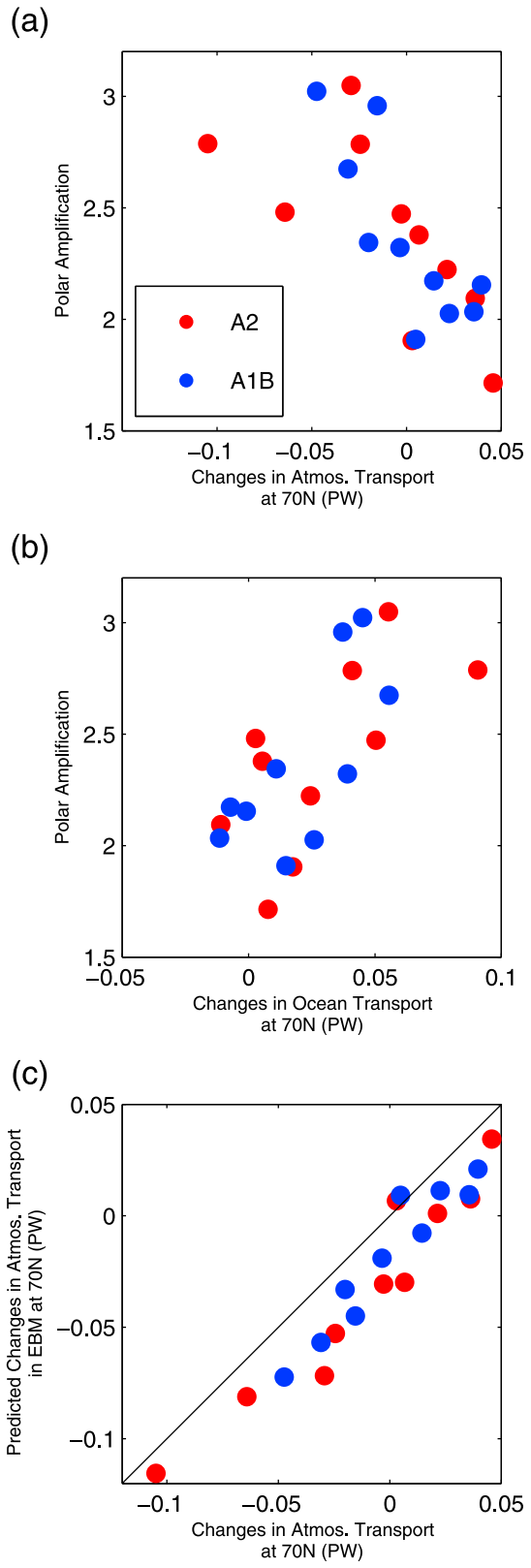

Figure 2. (a) Polar amplification versus changes in atmospheric energy transport at 70N. (b) Polar amplification versus changes in oceanic transport at 70N. (c) EBM predicted changes in atmospheric energy transport versus actual changes in atmospheric energy transport in the GCMs at 70N. Blue dots are from the A1B scenario, and red dots are from the A2 scenario.

transport dominates the spread of changes in the atmospheric energy transport (as discussed in section 2.1), and is anti-correlated with polar amplification. Polar amplification flattens the meridional temperature gradient and decreases the DSE transport. The spread of atmospheric energy transport cannot explain the spread of polar amplification; models with greater polar amplification must instead have stronger local feedbacks.

[9] The spread of atmospheric transport explains most of the spread in total transport (the correlation between the two transports is 0.75), thus, the correlation coefficient between the total transport and the 2 m air polar amplification is also negative.

[10] The changes in oceanic transport are positively correlated with the 2 m air polar amplification and sea ice loss (as shown in Figure 2b) [*Holland et al.*, 2006]. Enhanced ocean transport may cause temperature increases and accelerated ice melting [*Mahlstein and Knutti*, 2011]. The causality may be the opposite direction though; as multi-year ice is replaced by thinner first-year ice, the fast formation of ice may also trigger enhanced ocean transport [*Bitz et al.*, 2006]. It is also worth pointing out that much of the ocean energy transport increase happens at depth. *Bitz et al.* [2006] and S. J. Vavrus et al. (21st - century arctic climate change in CCSM4, submitted to *Journal of Climate*, 2011) show that the warming of the ocean is strongest at depth, not at the surface where it would affect sea ice. In addition, the surface Arctic ocean becomes fresher, which makes it increasingly difficult for the warming to be mixed upward due to increased stratification of the surface ocean.

3. Attribution of Changes in Atmospheric Energy Transport

[11] The results from Section 2 suggest a local diffusive relationship between atmospheric energy transport and temperature gradients [*North*, 1975]. In this section, we introduce an energy balance model (EBM) first used by *Hwang and Frierson* [2010] to help understand the coupling between local feedbacks and changes in atmospheric energy transport in CMIP3 GCMs. As we discussed later in this session, we utilize the EBM because its weak nonlinearity allows us to attribute the changes in energy transport to individual feedbacks. This EBM diffuses surface moist static energy (MSE) with a latitudinally uniform diffusivity that is the same for all models and in both time periods. Clear sky longwave radiation is parameterized as a linear function of temperature using a regression from the first 20 year period (2001 to 2020). The EBM is run with shortwave radiation, total surface flux, and longwave cloud radiative forcing as inputs to generate a mean climatology of the first 20 years. The model is then run under warmed conditions, with the enhanced greenhouse effect, shortwave radiation changes, longwave cloud radiative forcing changes, and surface flux changes. The model predicts energy transport, temperature, and clear sky longwave radiation in the two time periods. The EBM responds to a localized heating at a particular latitude with both a local increase in OLR and increased diffusive transport away, with the partition between the two determined by the diffusivity constant.

[12] Applied to the Arctic, the EBM captures the net effect of the two main mechanisms that influence atmospheric energy transport at around 70N: (1) increasing water vapor in the warmer climate leading to increasing moisture trans-

Table 2. Correlations Between Transports and Polar Amplification in the A1B and the A2 Scenarios Combined[a]

Changes in Northward Energy Transport at 70N	Changes in 2 m Temperature Poleward of 70N	Polar Amplification (2 m Temperature Poleward of 70N Divided by Global Mean)
Atmospheric Transport (DSE + Moisture)	**−0.61**	**−0.70**
DSE Transport	**−0.69**	**−0.72**
Moisture Transport	0.26	0.15
Ocean Transport	0.58	0.47
Total Transport (Atmospheric + Oceanic)	−0.32	−0.33

[a]The correlations that are significant (p value smaller than 0.01) are bold.

port, and (2) decreasing temperature gradients resulting from stronger positive feedbacks in the Arctic leading to decreased DSE transport.

[13] Figure 2c shows the predicted changes in the atmospheric energy transport at 70N in the EBM versus the actual changes in the GCMs. The EBM is able to explain much of the spread among individual GCMs (the correlation coefficient is 0.94). However, it tends to underestimate the surface trapped warming in the Arctic and predicts slightly too much equatorward transport.

[14] With the EBM, we can evaluate the influence of individual processes by prescribing the vertical flux perturbations they induce one at a time. The sum of these single-forcing EBM changes is nearly identical to the EBM-predicted change that considers the net changes in vertical fluxes from all processes at once (y axis in Figure 2c), with the difference of the two being less than 3% of the total predicted changes. Thus, we can quantitatively analyze which factors cause most of the change in atmospheric energy transport. For example, we first break down the predicted changes in atmospheric energy transport into two components, the changes due to a uniform increase of the greenhouse effect and the changes due to all other variations with latitudinal structure.

[15] The first term is G in Figure 3a, which is an increased atmospheric transport resulting from the enhanced greenhouse effect from CO_2. Each dot represents the result from one GCM. The CO_2 greenhouse effect is prescribed to be uniform across latitudes (see *Hwang and Frierson* [2010] for details), but the moisture content preferentially increases in low latitudes leading to an increase in the meridional MSE gradient, and thus a small increase in atmospheric transport at 70N. This term (G) is about 0.05 PW in all of the models, a similar value to the increasing moisture transport shown in Figure 1b.

[16] The second term is F in Figure 3a, which represents the change in atmospheric transport caused by all of the other vertical fluxes we prescribe, which are shortwave radiation changes at the top of the atmosphere, longwave cloud radiative forcing changes, and upward surface flux changes. It includes the effects of varying surface albedo, clouds, aerosol forcings, and ocean heat transport/storage. This term F is negative in all of the GCMs, because the net effect of these variations amplifies the Arctic warming, which weakens the equator-to-pole MSE gradient and results in a decrease in atmospheric transport. It also explains much of the wide range of the decreasing DSE transport in Figure 1b. The color of the dots is in the same order as in Figure 1.

[17] We can further break down the term F in Figure 3a into two parts: the part that is influenced by the vertical flux perturbations poleward of 70N (Figure 3b) and the part that is influenced by perturbations southward of 70N, from the South Pole to 70N (Figure 3c). For these two regions, we again break down the perturbations into six components that are associated with: (1) the surface albedo effect (I), (2) the cloud SW effect (C_S), (3) the cloud LW effect (C_L), (4) the non-cloud (atmospheric) SW absorption effect (N_A) which is associated with increasing black carbon, CO_2, and water vapor in the future, (5) non-cloud (atmospheric) SW scattering (N_S) which is associated with decreasing sulfate aerosol, and (6) ocean (O) which is associated with changes in surface fluxes. (See *Taylor et al.* [2007] and *Hwang and Frierson* [2010] for detailed explanations of how to separate these components.) Results from these single-forcing EBM experiments are plotted in Figures 3b and 3c. For example, I in Figure 3b demonstrates the EBM-predicted changes in atmospheric energy transport when we prescribe the surface albedo effects poleward of 70N in each GCM, each dot representing one model.

[18] The surface albedo effect in the Arctic accounts for a significant amount of the decrease in atmospheric transport (I in Figure 3b). It also explains some model-to-model spread as dots are stacked red to blue from top to bottom.

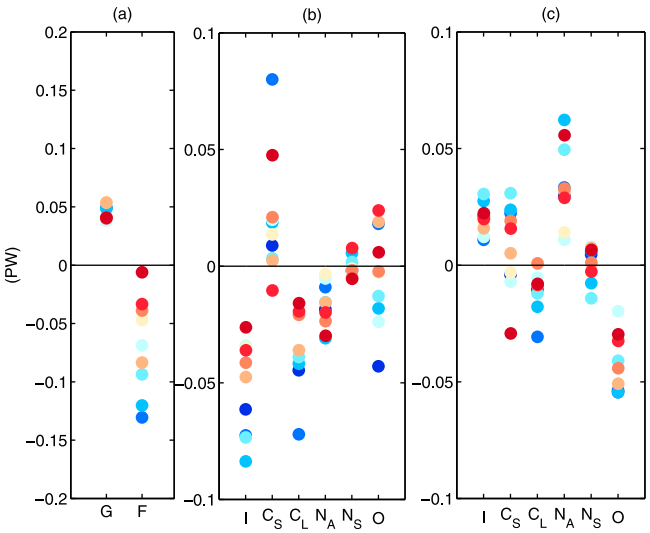

Figure 3. Attribution of changes in poleward atmospheric energy transport (in PW) at 70N in the A2 scenario. (a) Enhanced greenhouse effect (G) and all other forcings (F) at all latitudes. (b) Surface albedo (I), cloud shortwave (C_S) and cloud longwave (C_L), clear-sky absorption (N_A), clear-sky scattering (N_S), and ocean heat transport for latitudes poleward of 70N. (c) As in Figure 3b for latitudes between the South Pole and 70N. The color of the dots is in the same order as in Figure 1.

The surface albedo effect results in less decrease in transport in red models, which are the models that project increasing transport. This result also indicates that models that project more ice melting are the models that show decreasing energy transport (blue models), which are also the models that have higher polar amplification (Figure 2a).

[19] Similar feature are present for the longwave cloud effect and ocean effect (C_L and O in Figure 3b). Enhanced warming caused by the longwave cloud effect and surface fluxes in the Arctic explain some of the model-to-model spread in atmospheric transport.

[20] The cooling effect from shortwave clouds, due to increased cloud coverage in the Arctic with warming, leads to increased energy transport (C_S in Figure 3b). It also contributes to a large amount of the model spread. Interestingly, it is not stacked from red to blue or blue to red, which implies there is little correlation between atmospheric transport and the SW cloud effect.

[21] Vertical fluxes outside the Arctic also have an effect on atmospheric energy transport. Decreasing snow cover in NH land results in increasing poleward atmospheric transport at 70N (I in Figure 3c). Increasing black carbon and water vapor in low latitudes serves as a heating source in midlatitudes and the tropics and results in enhanced poleward atmospheric transport at 70N (N_A in Figure 3c). Weaker overturning circulation in North Atlantic weakens the ocean energy transport in midlatitudes, which also have a weakening effect on atmospheric transport at 70N (O in Figure 3c).

4. Concluding Remarks

[22] Previous studies have shown that increasing energy transports can contribute to sea ice melting and Arctic warming, even in the absence of surface albedo feedback. To understand to what extent energy transport can contribute to polar amplification, we investigate the relationships between energy transports and the local feedback processes in the Arctic across a group of CMIP3 models. We find that positive feedbacks in the Arctic have a significant influence on decreasing DSE transport, which offsets the increase in moisture transport and oceanic transport. As a result, models with larger positive feedbacks have higher amplification but decreased horizontal energy input (total energy transport). The increase in water vapor transport causes a small systematic warming of higher latitudes but does not explain the spread in surface polar amplification. While this paper focuses on explaining the poleward energy transports in the atmosphere, we find it likely that differences in local feedbacks also explain the range of polar amplification, in accordance with previous results [*Hall*, 2004; *Winton*, 2006; *Boe et al.*, 2009].

[23] We have shown that transport into the Arctic is essentially linearly proportional to moist static energy gradients. Therefore, positive feedback processes that amplify polar warming also decrease energy transport into the high latitudes. This negative feedback on polar amplification should be taken into account when interpreting simulations of global warming or results of fixed feedback experiments. We believe that the use of EBMs or alternative energy transport attribution methods can be useful for interpreting such experiments.

[24] **Acknowledgments.** We thank Cecilia Bitz and Brian Rose for valuable discussions and two anonymous reviewers for constructive comments. We acknowledge support from NSF grants ATM-0846641 and ATM-0936059. We acknowledge the modeling groups, the Program for Climate Model Diagnosis and Intercomparison (PCMDI) and the WCRP's Working Group on Coupled Modelling (WGCM) for their roles in making available the WCRP CMIP3 multi-model dataset. Support of this dataset is provided by the Office of Science, U.S. Department of Energy.

[25] The Editor thanks the two anonymous reviewers for their assistance in evaluating this paper.

References

Alexeev, V., P. Langen, and J. Bates (2005), Polar amplification of surface warming on an aquaplanet in "ghost forcing" experiments without sea ice feedbacks, *Clim. Dyn.*, *24*(7), 655–666.

Bitz, C., P. Gent, R. Woodgate, M. Holland, and R. Lindsay (2006), The influence of sea ice on ocean heat uptake in response to increasing CO_2, *J. Clim.*, *19*(11), 2437–2450.

Boe, J., A. Hall, and X. Qu (2009), Current gcms unrealistic negative feedback in the arctic, *J. Clim.*, *22*(17), 4682–4695.

Cunningham, S. A., and R. Marsh (2010), Observing and modeling changes in the Atlantic MOC, *Wiley Interdiscip. Rev. Clim. Change*, *1*(2), 180–191.

Graversen, R. G., and M. Wang (2009), Polar amplification in a coupled climate model with locked albedo, *Clim. Dyn.*, *33*(5).

Gregory, J. M., et al. (2005), A model intercomparison of changes in the Atlantic thermohaline circulation in response to increasing atmospheric CO_2 concentration, *Geophys. Res. Lett.*, *32*, L12703, doi:10.1029/2005GL023209.

Hall, A. (2004), The role of surface albedo feedback in climate, *J. Clim.*, *17*(7), 1550–1568.

Held, I. M., and B. J. Soden (2006), Robust responses of the hydrological cycle to global warming, *J. Clim.*, *19*(21), 5686–5699.

Holland, M., and C. Bitz (2003), Polar amplification of climate change in the coupled model intercomparison project, *Clim. Dyn.*, *21*, 221–232.

Holland, M. M., C. M. Bitz, and B. Tremblay (2006), Future abrupt reductions in the summer Arctic sea ice, *Geophys. Res. Lett.*, *33*, L23503, doi:10.1029/2006GL028024.

Holland, M. M., M. C. Serreze, and J. Stroeve (2010), The sea ice mass budget of the Arctic and its future change as simulated by coupled climate models, *Clim. Dyn.*, *34*, 185–200.

Hwang, Y.-T., and D. M. W. Frierson (2010), Increasing atmospheric poleward energy transport with global warming, *Geophys. Res. Lett.*, *37*, L24807, doi:10.1029/2010GL045440.

Hwang, Y.-T., D. M. W. Frierson, B. J. Soden, and I. M. Held (2011), Corrigendum, *J. Clim.*, *24*(5), 1559–1560.

Intergovernmental Panel on Climate Change (2007), *Climate Change* 2007*: The Physical Science Basis. Contribution of Working Group I the Fourth Assessment Report of the Intergovernmental Panel on Climate Change*, edited by S. Solomon et al., Cambridge Univ. Press, Cambridge, U. K.

Mahlstein, I., and R. Knutti (2011), Ocean heat transport as a cause for model uncertainty in projected arctic warming, *J. Clim.*, *24*(5), 1451–1460.

Manabe, S., and R. J. Stouffer (1980), Sensitivity of a global climate model to an increase of CO_2 concentration in the atmosphere, *J. Geophys. Res.*, *85*(C10), 5529–5554.

North, G. R. (1975), Theory of energy-balance climate models, *J. Atmos. Sci.*, *32*, 2033–2043.

Overland, J. E., P. Turet, and A. H. Oort (1996), Regional variations of moist static energy flux into the Arctic, *J. Clim.*, *9*(1), 54–65.

Sellers, W. D. (1969), A global climatic model based on energy balance of the Earth-atmosphere system, *J. Appl. Meteorol.*, *8*, 392–400.

Solomon, A. (2006), Impact of latent heat release on polar climate, *Geophys. Res. Lett.*, *33*, L07716, doi:10.1029/2005GL025607.

Taylor, K. E., M. Crucifix, P. Braconnot, C. D. Hewitt, C. Doutriaux, A. J. Broccoli, J. F. B. Mitchell, and M. J. Webb (2007), Estimating shortwave radiative forcing and response in climate models, *J. Clim.*, *20*(11), 2530–2543.

Trenberth, K. E., and J. T. Fasullo (2010), Simulation of present-day and twenty-first-century energy budgets of the southern oceans, *J. Clim.*, *23*, 440–454.

Winton, M. (2006), Amplified Arctic climate change: What does surface albedo feedback have to do with it?, *Geophys. Res. Lett.*, *33*, L03701, doi:10.1029/2005GL025244.

D. M. W. Frierson and Y.-T. Hwang, Department of Atmospheric Sciences, University of Washington, 408 ATG Bldg., Box 351640, Seattle, WA 98195, USA. (dargan@atmos.washington.edu; yting@atmos.washington.edu)

J. E. Kay, Climate and Global Dynamics Division, National Center for Atmospheric Research, PO Box 3000, Boulder, CO 80307, USA. (jenkay@ucar.edu)